Proc. Natl. Acad. Sci. USA
Vol. 93, pp. 6907–6912, July 1996
Biochemistry

Mutational analysis and molecular modeling of the nonapeptide hormone binding domains of the [Arg^8]vasotocin receptor

(*Catostomus commersoni*/isotocin receptor/vasopressin receptor/oxytocin receptor/neuropeptide)

HOLGER HAUSMANN*, ANKE RICHTERS*, HANS-JÜRGEN KREIENKAMP*, WOLFGANG MEYERHOF†, HENRI MATTES‡, KARL LEDERIS§, HENK ZWIERS§, AND DIETMAR RICHTER*¶

*Institut für Zellbiochemie und klinische Neurobiologie, Universität Hamburg, Martinistrasse 52, 20246 Hamburg, Germany; †Abteilung für Molekulare Genetik, Deutsches Institut für Ernährungsforschung, Universität Potsdam, Arthur-Scheunert-Allee 114–116, 14558 Potsdam-Rehbrücke, Germany; ‡Preclinical Research, Sandoz Pharma Ltd., 4002 Basle, Switzerland; and §Department of Pharmacology and Therapeutics, Faculty of Medicine, The University of Calgary, Calgary, AB, Canada T2N 4N1

Communicated by B. Sakmann, Max-Planck-Institut für Medizinische Forschung, Heidelberg, Germany, April 8, 1996 (received for review March 7, 1996)

ABSTRACT **To identify determinants that form nonapeptide hormone binding domains of the white sucker *Catostomus commersoni* [Arg^8]vasotocin receptor, chimeric constructs encoding parts of the vasotocin receptor and parts of the isotocin receptor have been analyzed by [(3,5-^{3}H)Tyr^2, Arg^8]vasotocin binding to membranes of human embryonic kidney cells previously transfected with the different cDNA constructs and by functional expression studies in *Xenopus laevis* oocytes injected with mutant cRNAs. The results indicate that the N terminus and a region spanning the second extracellular loop and its flanking transmembrane segments, which contains a number of amino acid residues that are conserved throughout the nonapeptide receptor family, contribute to the affinity of the receptor for its ligand. Nonapeptide selectivity, however, is mainly defined by transmembrane region VI and the third extracellular loop. These results are complemented by a molecular model of the vasotocin receptor obtained by aligning its sequence with those of other G-protein coupled receptors as well as that of bacteriorhodopsin. The model indicates that amino acid residues of transmembrane regions II–VII that are located close to the extracellular surface also contribute to the binding of vasotocin.**

A number of heptahelical G-protein coupled receptor subtypes of the nonapeptide vasopressin (VP)/oxytocin (OT) family have been characterized by pharmacological studies (1) as well as by molecular cloning experiments (2–10). These subtypes are activated differently by several natural (11, 12) and synthetic (13, 14) nonapeptide agonists. Comparison of the amino acid sequences of the oxytocin (2, 3), isotocin (IT) (4), vasopressin V_{1a} (5, 6), [Arg^8]vasotocin (VT) (7), and vasopressin V_{1b} (8) and V_2 receptors (3, 9, 10) has revealed that they form a subfamily within the superfamily of G-protein coupled receptors. The greatest similarities exist within the putative transmembrane regions (TMs), as has been observed in other G-protein coupled receptor subfamilies (15). However, conserved amino acid residues are also present in nonapeptide receptors in the first and second, but not the third, extracellular loop and in those parts of the TMs that are close to the extracellular surface. Because these residues are not conserved in other heptahelical receptors, it has been suggested that they are involved in the formation of peptide binding pockets (16). This suggestion is supported by mutational analyses of other neuropeptide receptors where it has been shown that the extracellular loops contribute to ligand binding (reviewed in refs. 17 and 18).

Here we report on studies of ligand binding to the fish *Catostomus commersoni* VT receptor (VTR). While the VTR discriminates well between IT and VT, which are the OT and [Arg^8]vasopressin homologues in teleosts, the IT receptor (ITR) shows little preference for one over the other (4, 7). To investigate which parts of the VTR are involved in ligand binding, various chimeras consisting of parts of the VTR and parts of the ITR have been constructed and expressed either in human embryonic kidney (HEK) cells or *Xenopus laevis* oocytes. The results presented here show that at least three different regions of the VTR participate in VT binding. The data are consistent with a molecular model based on the VTR sequence.

MATERIALS AND METHODS

Materials. [(3, 5-^{3}H)Tyr^2, Arg^8]vasotocin (specific activity 16 Ci/mmol; 1 Ci = 37 GBq) was purchased from DuPont.

Construction of Mutants. To exchange parts of the VTR and the ITR, restriction sites were introduced into appropriate positions of the VTR or ITR cDNAs; these were located as indicated in Fig. 1. Individual cDNA fragments were amplified by using a thermophilic DNA polymerase (Ventpolymerase; New England Biolabs) using primers specific for either the 5′ or 3′ parts of the nonapeptide receptor cDNAs and internal mutagenic primers. Amplified DNA fragments that overlapped at the introduced restriction sites were cut with the appropriate endonuclease, ligated, and cloned into either pBluescript or pcDNA3. The correct construction of the chimeras was confirmed by automated DNA sequence analysis (Applied Biosystems model 373 A).

Ligand Binding Assays. HEK cells were transfected by the calcium phosphate precipitation method (20) and selected in media containing 450 μg of G418 per ml. For [(3,5-^{3}H)Tyr^2, Arg^8]vasotocin binding, 30 μg of membrane proteins was incubated at 26°C for 45 min with various concentrations of the radioligand in 100 μl binding buffer (3).

Functional Expression Assays in Oocytes. Plasmids, which were linearized in the polylinker region, served as templates for the synthesis of *in vitro* transcribed cRNAs by using a T7 RNA polymerase transcription kit (Promega). Injection of cRNAs into frog oocytes and voltage-clamp measurements were performed as described (7).

Molecular Modeling. The sequences of the VTR and ITR and the rat V_{1a} receptor were aligned with those of the somatostatin and serotonin receptors as well as with that of bacteriorhodopsin. The precise locations of the first and last amino acids of the TMs were determined by comparison with

The publication costs of this article were defrayed in part by page charge payment. This article must therefore be hereby marked "*advertisement*" in accordance with 18 U.S.C. §1734 solely to indicate this fact.

Abbreviations: HEK cells, human embryonic kidney cells; IT, isotocin; ITR, isotocin receptor; OT, oxytocin; TM, transmembrane region; VP, vasopressin; VT, [Arg^8]vasotocin; VTR, [Arg^8]vasotocin receptor

¶To whom reprint requests should be addressed.

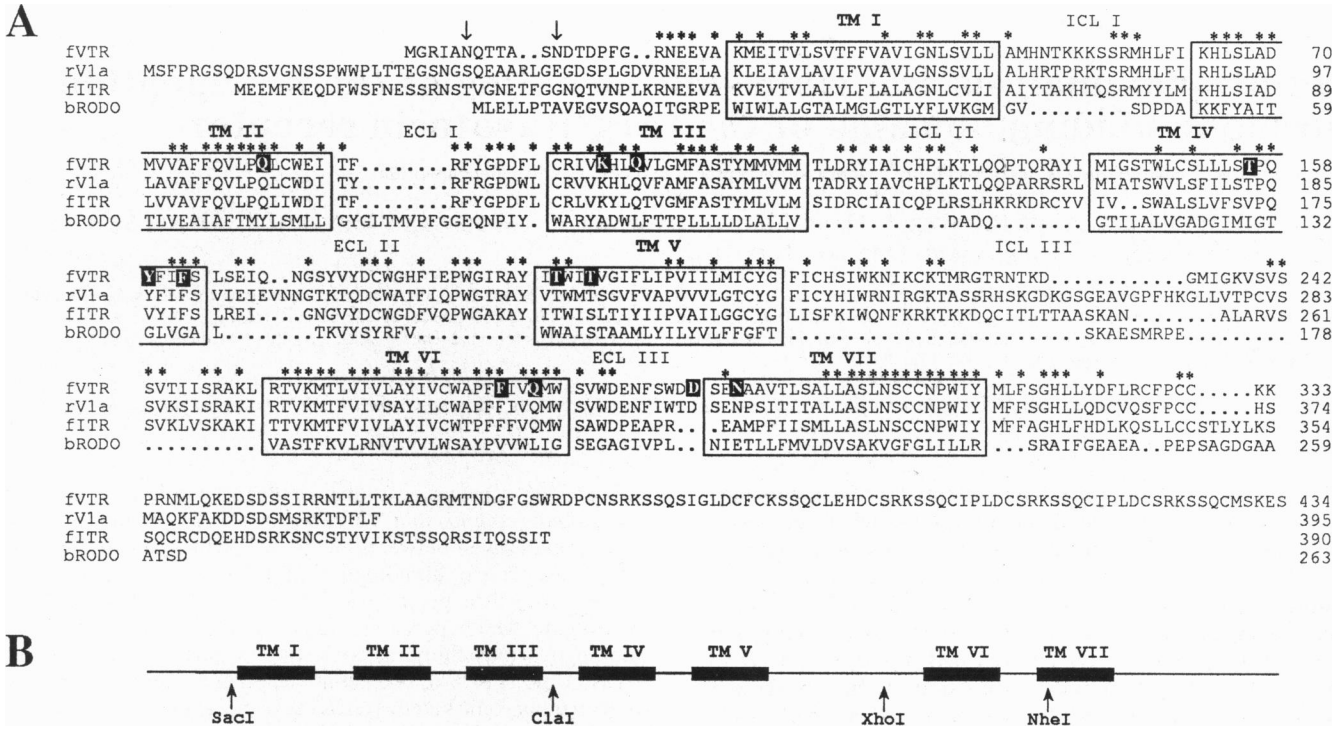

FIG. 1. (*A*) Amino acid sequence alignment of the VTR and ITR from the fish (f) *Catostomus commersoni* (4, 7), the rat V_{1a} receptor, rV1a (5), and bacteriorhodopsin (bRODO) (19). The sequences have been aligned by using the PILEUP algorithm (Genetics Computer Group, Madison, WI). Gaps have been introduced to maximize homology. Transmembrane regions (TMs) are boxed and have been defined as outlined in the *Materials and Methods*. Residues that are conserved between the three receptors are marked by an asterisk. Residues that may be involved in VT binding to the VTR are shown in white letters. Potential N-linked glycosylation sites are indicated by arrows. On the right hand side of the figure, the numbering of the amino acids is indicated. ECL, extracellular loop; ICL, intracellular loop. (*B*) Schematic structure of a nonapeptide receptor showing the positions of the introduced cleavage sites (see *Materials and Methods*).

an alignment table previously obtained for roughly thirty different G-protein coupled receptors (19).

The transmembrane sequences of bacteriorhodopsin were changed to those of the fish VTR by using the biopolymer module of SYBYL (Tripos Associates, St. Louis). A template was constructed for helical proline residues by combining residues 38–63 and 80–101 from helices 2 and 3, respectively (the numbering refers to the bacteriorhodopsin sequence shown in Fig. 1), as reported (21). Backbone angles of the sequences containing proline residues either in the middle of a helix or near the binding pocket were adjusted to those found in the template. Helices 2 to 6 were changed accordingly.

After removal of steric conflicts between side chains of neighboring helices "by hand," an energy minimization of the seven-helix model was started, 2000 iterations of conjugate gradient minimization with all C^{α}s fixed at their original positions, to optimize the side chain orientations (MAXIMIN, SYBYL). A model of [Arg^8]vasotocin forming an ideal type II β turn at position Ile^3–Gln^4, with the Pro^7-Arg^8-Gly^9 sequence of the nonapeptide in an extended conformation, was built and energy optimized without constraints. This model was docked manually into the putative binding site between helices 3 and 7. Several different docking positions were studied and analyzed. The complex with the best interactions was finally minimized by using the ANNEAL module of SYBYL.

RESULTS AND DISCUSSION

Comparison of the nonapeptide receptor sequences from the rat and fish indicates a significant number of conserved amino acid residues, particularly in the first two extracellular loops and in those regions of the transmembrane segments which are close to the extracellular surface (Fig. 1). Because these residues are not conserved in other heptahelical receptors, they may contribute to the formation of peptide binding domains (16). To identify sequence elements of the VTR that are responsible for the binding of the ligand, chimeras between the VTR and the ITR were constructed and analyzed for their ability to bind [(3,5-^{3}H)Tyr^2, Arg^8]vasotocin in HEK cells transfected with the various cDNAs. In parallel experiments,

Table 1. IC_{50} and threshold values for VT and IT

Receptor type	VT, nM			IT, nM	
	K_D	IC_{50}	Threshold	IC_{50}	Threshold
VTR wildtype	0.06	3.6	0.03	$>10^3$	120
ITR wildtype	7.10	38.4	2.0	2.57	1.9
ITR / VTR 1	0.22	6.9	0.1	$>10^3$	120
ITR / VTR 2	–	–	2000	–	$>10^5$
ITR / VTR 3	0.77	8.6	2.0	$>10^3$	2000
ITR / VTR 4	2.10	16.9	39	3.32	8
ΔN VTR	1.46	9.4	8.0	$>10^3$	$>10^5$

Shown are IC_{50} and threshold values for the ligands VT and IT at the wild-type VTR and ITR, the constructed chimeras ITR/VTR 1–4, and the deletion mutant ΔN VTR. K_D values were obtained from saturation experiments using [^{3}H]VT (0.03–20 nM) and calculated by Scatchard plot analysis. IC_{50} values were obtained by displacement of [^{3}H]VT as described. A threshold value is the lowest concentration of ligand that gives a response in voltage-clamped frog oocytes injected with *in vitro* transcribed RNAs for either wild-type or chimeric receptors and is indicative of the potency of VT or IT at its receptor. –, No measurable binding.

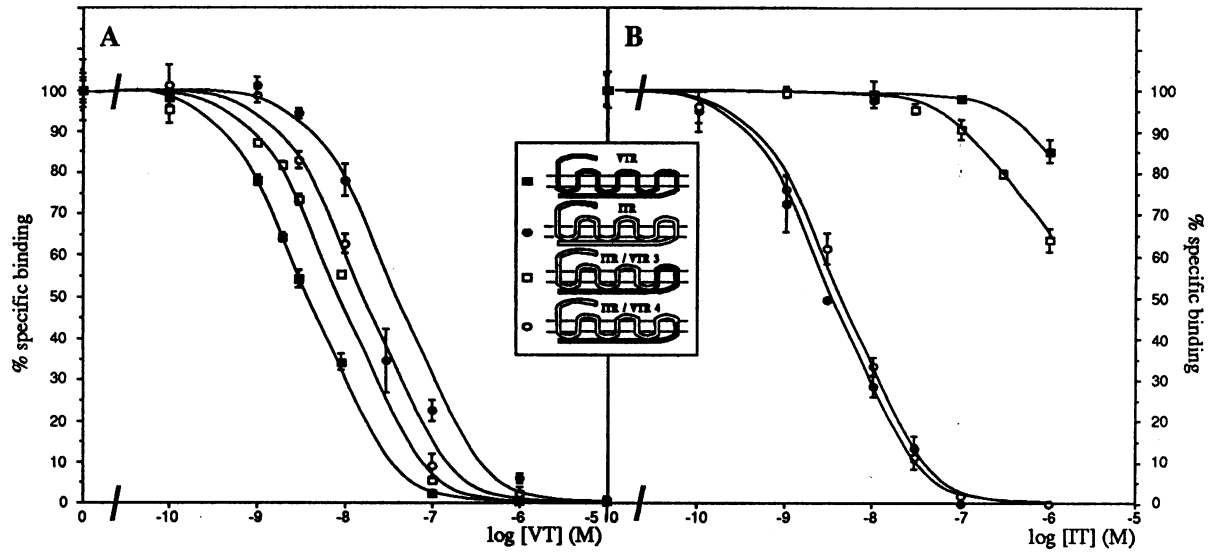

FIG. 2. Comparison of the binding properties of the wild type VTR and ITR and of chimeras ITR/VTR 3 and 4 in membrane preparations of transfected HEK cells. The figure shows the competition of [^{3}H]vasotocin (1 nM) with increasing concentrations of VT (*A*) and IT (*B*). Nonspecific binding was determined in the presence of 10 μM VT.

cRNAs were injected into frog oocytes for functional expression studies. As illustrated in Table 1 four chimeras (ITR/VTR 1–4) were studied in which segments of the native VTR were systematically exchanged for the corresponding segments of the ITR; the four chimeras were ITR/VTR 1 (ITR_{1-41}/VTR_{24-434}), ITR/VTR 2 (ITR_{1-141}/$VTR_{123-434}$), ITR/VTR 3 (ITR_{1-267}/$VTR_{249-434}$), and ITR/VTR 4 (ITR_{1-318}/$VTR_{303-434}$). In addition, a mutant was made (ΔN-VTR) that lacks the N terminus of the native VTR up to Arg^{19}, which includes all of the asparagine-linked glycosylation sites, and contains instead the artificial N terminus MVATGAQLEFGT.

Binding and Functional Expression Studies. Fig. 2 and Table 1 show the competition binding of unlabeled VT and IT with radiolabeled VT to membrane fractions prepared from HEK cells transfected with the various cDNA constructs. The native VTR has a significantly higher binding preference for VT (IC_{50} = 3.6 nM) than for IT ($IC_{50} > 10^3$ nM); the native ITR, on the other hand, has only an ≈10-fold higher preference for IT (IC_{50} = 2.5 nM) than for VT (IC_{50} = 38.4 nM). Similar results were obtained from functional expression studies in voltage-clamped frog oocytes. The threshold concentrations of VT and IT that induced a significant membrane current of 1–5 nA in *X. laevis* oocytes injected with VTR RNA were 0.03 nM and 120 nM, respectively (Table 1). In contrast, the ITR displays almost identical threshold values for IT (1.9 nM) and VT (2.0 nM). The competition studies, the functional expression data and the apparent binding constants for VT confirm that the VTR is highly selective for VT, whereas the ITR is activated by almost identical concentrations of VT and IT (Table 1).

The mutant construct ITR/VTR 1, which contains the extracellular N terminus of the ITR, was comparable to the native VTR in terms of radioligand binding and threshold activation in injected oocytes (Table 1). In contrast, the ΔN VTR mutant, which lacks potential N-terminal glycosylation sites, displayed a significant reduction in the binding of labeled [Arg^8]vasotocin and an increase in the threshold concentration for activation by VT, suggesting that this region of the VTR contains residues that contribute to VT binding (Table 1). These reductions in binding and function are not due to reduced biosynthesis of the VTR in either cell system because functional expression studies in frog oocytes showed that the maximal amplitudes of the induced membrane currents were similar for the ΔN VTR mutant and the native VTR; immu-

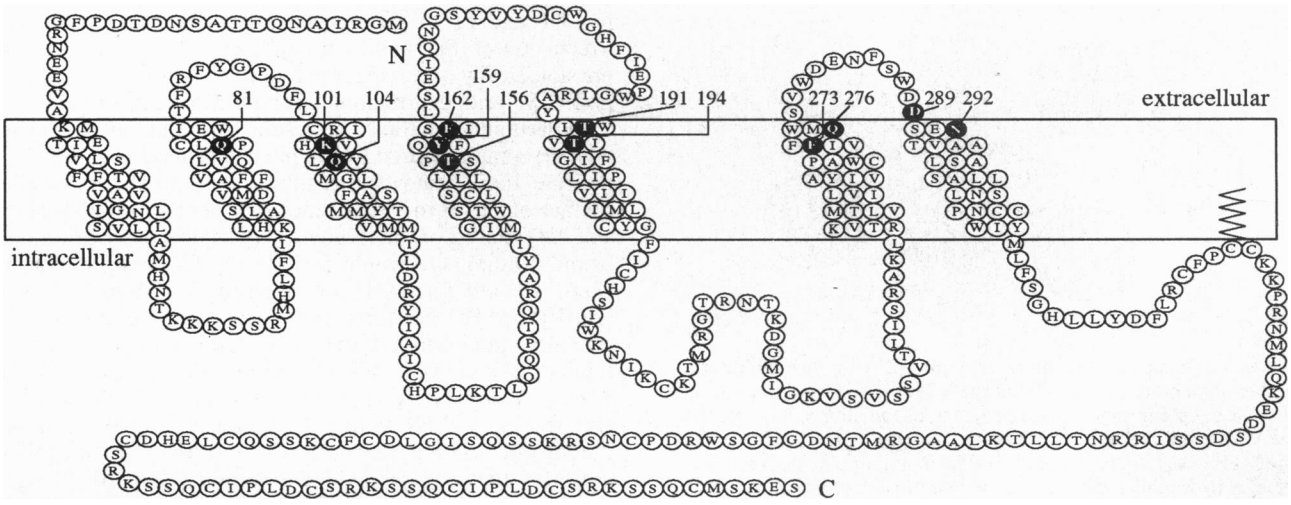

FIG. 3. Scheme of the *C. commersoni* VTR showing the seven putative membrane-spanning domains and amino acid residues (in white letters) that may contribute to VT binding (see also Fig. 1). ξ, The putative palmitoylation site.

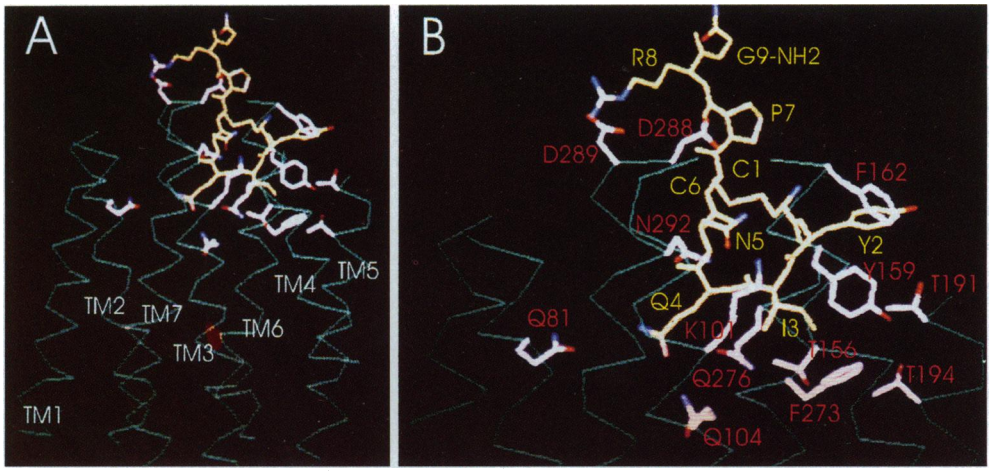

FIG. 4. Three-dimensional model of the VTR with VT docked in the binding pocket. (*A*) Lateral view showing the seven transmembrane helices by their α-traces (green). The peptide ligand is shown in yellow; N and O are blue and red, respectively. All side chains of amino acid residues in the receptor that are located within a distance of 5 Å of the ligand are displayed in pink. (*B*) Magnification of the upper part of the model. Amino acid residues (single letter code) of VT are numbered in yellow, and those of the receptor contributing to binding are in red.

nocytochemical analysis also revealed that the truncated VTR protein is targeted normally to the plasma membrane of HEK cells (data not shown). Moreover, the N terminus also appears to contain residues that affect peptide selectivity. This is supported by the observation that the ability of a mutant VTR to bind VT is almost normal when the N terminus is replaced by the corresponding rat V_{1a} vasopressin receptor segment (data not shown) and by the high threshold concentration of IT observed for the ΔN VTR mutant (Table 1).

When sequences up to the second intracellular loop of the VTR were replaced by the corresponding ITR sequence (ITR/VTR 2), neither a K_D nor an IC_{50} value was measurable in the radioligand binding assay; in the functional expression assay, the threshold concentration of VT increased to 2×10^3 nM (Table 1). Because the mutant receptor protein was not detectable in mammalian cell membranes either by Western blotting or by fluorescence microscopy (data not shown), the data suggest that this chimeric construct lacks the correct start–stop–transfer signal sequences that are known to be required for the correct insertion of polypeptide chains into the membrane of the endoplasmic reticulum (22–24).

In contrast to ITR/VTR 2, the chimeric receptor ITR/VTR 3 in which sequences up to the sixth transmembrane domain of the VTR were replaced by the corresponding segment of the ITR showed improved activities in the binding and functional assays. As shown in Fig. 2*A* this mutant construct binds VT with properties in between those of the native VTR and ITR. With respect to IT binding, the mutant resembles the native VTR (Fig. 2*B*). In the functional assay, ITR/VTR 3 displayed a greater (about 1000-fold) preference for VT over IT (Table 1). Apparently the second extracellular loop and the adjacent TMs contain determinants that contribute significantly to the affinity but not to the specificity of the binding of the two nonapeptides to the VTR. It is plausible that these determinants could interact with the conserved parts of nonapeptides such as the C-terminal amide, the ring structure, or the invariant amino acid residues. Direct proof of the involvement of the first extracellular loop in peptide hormone binding has been obtained for the bovine renal V_2 vasopressin receptor (3, 25) by photoaffinity labeling with a vasopressin agonist and by mutational analysis. In the latter case, Asp-103 in the first extracellular loop appears to be directly involved in agonist binding (26). This observation is substantiated by the finding that, in the rat V_{1a} receptor, a tyrosine in the position corresponding to Asp-103 is responsible for high affinity agonist binding (27).

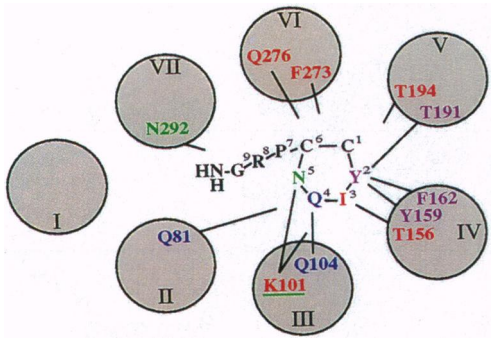

FIG. 5. Scheme of the interaction of VT with the membrane-spanning domains (circles I–VII) of the VTR viewed from the surface of the plasma membrane. The numbering of the amino acid residues of the VTR is according to that depicted in Fig. 1. Amino acid residues of the VTR (single letter code) in red form a lipophilic pocket; those in blue, a hydrophilic cleft; those involved in hydrogen bonding are given in green; and those in specific stacking interaction, in purple. Underlining of amino acid K101 indicates that it is also involved in hydrogen bonding.

The chimera containing only TM VII and the cytoplasmic tail of the VTR (ITR/VTR 4) resembles the ITR (Fig. 2 and Table 1). The mutant receptor and the ITR are similar in their binding properties for VT and IT and display similar potencies for VT and IT in the oocyte, indicating that determinants which confer the ability to differentiate between the two physiologically occurring nonapeptides in teleosts are located in TM VI and/or the nonconserved third extracellular loop.

Molecular Modeling. The results from the mutational analysis are complemented by the molecular modeling data which indicate that amino acid residues close to the extracellular surface of TM II to VII interact with peptide agonists (Figs. 3 and 4*A*). Based on the model, a molecular description of the ligand binding site would include the following interactions (Figs. 4*B* and 5): (*i*) The conserved Gln-81 in TM II and Gln-104 in TM III form part of a hydrophilic cleft which accommodates Gln-4 of the VT with the strongest interaction taking place between VT–Gln-4 and Gln-104. Mutating Gln-104 to a leucine residue resulted in a mutant VTR that is not able to bind VT supporting the importance of this residue in the ligand binding reaction (Fig. 6). (*ii*) The model also indicates that the methylene groups of Lys-101 (TM III), residues Thr-156 (TM IV), Thr-194 (TM V), and Phe-273 (TM VI), and the methylene groups of Gln-276 (TM VI) point into the binding site and define a lipophilic pocket into which Ile-3

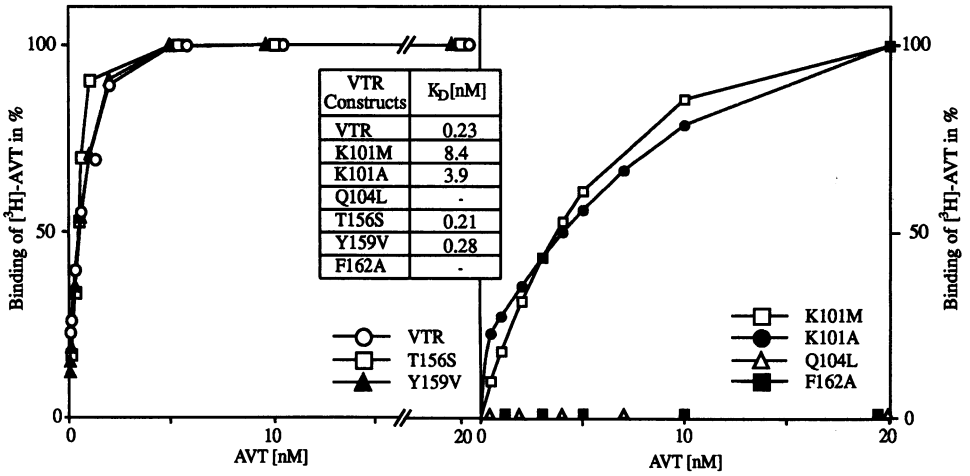

FIG. 6. Comparison of the binding properties of wild-type and mutant vasotocin receptors. Mutant VTRs were generated by PCR-mediated site-directed mutagenesis (28), and their correct sequences confirmed by automated DNA sequence analysis. Specific binding of [^{3}H]vasotocin to membranes prepared from HEK cells transfected with the appropriate receptor cDNAs is shown as the percentage of maximum binding. K_D values were obtained from saturation experiments using 0.06–20 nM [^{3}H]VT and calculated by Scatchard plot analysis. –, No detectable binding. Amino acid residues are denoted by the single letter code.

of the VT docks (Figs. 4*B* and 5). Tyr-2 of VT has a specific stacking interaction with Tyr-159 (TM IV) and Phe-162 (TM IV) that is reinforced by hydrogen bonding with Thr-191 (TM V). Another important interaction takes place through a hydrogen bond between Lys-101 (TM III) and Asn-5 of the VT. Mutation of Lys-101 (TM III) into either a methionine or alanine residue resulted in a reduction, that of Phe-162 (TM IV) into an alanine in a complete loss in VT binding, indicating that both residues are crucial for ligand binding; in contrast, little or no reduction in ligand binding was observed when Thr-156 (TM IV) and Tyr-159 (TM IV) were mutated into a serine and valine, respectively (Fig. 6). (*iii*) On the opposite side of the nonapeptide, the backbone NH of Asn-5 makes another hydrogen bond with Asn-292 (TM VII). (*iv*) Finally, Arg-8 of the VT extends into the outermost regions of TM II and TM VII where it is anchored by Asp-289 (TM VII), thus positioning the agonist in its binding pocket in the interior of the TM segments. That Asp-289 contributes significantly to VT binding is in line with preliminary data obtained for a mutant construct lacking this residue which exhibits impaired binding to and activation by VT and IT.

The model also implies that several residues of the ligand interact with amino acids that are located in different TM segments—i.e., Tyr-2 of the ligand interacts with residues in TM IV and V; Ile-3 with residues in TM III, IV, V and VI; Gln-4 with residues in TM II and III; and Asn-5 with residues in TM III and VII (Fig. 5). Although the model does not include the extracellular loops, it shows that the side chain of Arg-8 of the VT is positioned close to the first extracellular loop. In the case of the vasopressin V_{1a} and V_2 receptors, this loop contains determinants that bind Arg-8 of vasopressin (25–27, 29).

Taken together, the results indicate that at least three different regions (N terminus; TM IV and V, second extracellular loop; TM VI, third extracellular loop) of the VTR participate in ligand binding. The first two regions mainly determine peptide potency and affinity probably by recognizing conserved amino acid residues of the nonapeptides. The third region, TM VI and the third extracellular loop, is likely to recognize nonapeptide specific structures and thereby determine peptide selectivity. This is reminiscent of the tachykinins and their receptors. In this case structural analyses have shown that the conserved C terminus of the tachykinins is required for agonist activity at all three receptor subtypes (30). Mutations introduced into the N terminus and the first and second extracellular loops severely impaired substance P binding to the substance P (NK_1) receptor (31, 32).

We thank Hans-Hinrich Hönck and Günter Ellinghausen for expert technical assistance, Dr. Mark Darlison for critically reading the manuscript, Helen Wilson of Nanton (Alberta) for help in the collection of *C. commersoni*, and the International Human Frontier Science Program (RG-84/94B) for financial support. The data presented are part of theses by H.H. and A.R.

1. Jard, S., Barberis, C., Audigier, S. & Tribollet, E. (1987) in *Progress in Brain Research*, eds. de Kloet, E. R., Wiegant, V. M. & de Wied, D. (Elsevier, Amsterdam), pp. 173–187.
2. Kimura, T., Tanizawa, O., Mori, K., Brownstein, M. J. & Okayama, H. (1992) *Nature (London)* **356,** 526–529.
3. Gorbulev, V., Buchner, H., Akhundova, A. & Fahrenholz, F. (1993) *Eur. J. Biochem.* **215,** 1–7.
4. Hausmann, H., Meyerhof, W., Zwiers, H., Lederis, K. & Richter, D. (1995) *FEBS Lett.* **370,** 227–230.
5. Morel, A., O'Carroll, A.-M., Brownstein, M. J. & Lolait, S. J. (1992) *Nature (London)* **356,** 523–526.
6. Thibonnier, M., Auzan, C., Madhun, Z., Wilkins, P., Berti-Mattera, L. & Clauser, E. (1994) *J. Biol. Chem.* **269,** 3304–3310.
7. Mahlmann, S., Meyerhof, W., Hausmann, H., Heierhorst, J., Schönrock, C., Zwiers, H., Lederis, K. & Richter, D. (1994) *Proc. Natl. Acad. Sci. USA* **91,** 1342–1345.
8. Sugimoto, T., Saito, M., Watanabe, Y., Hashimoto, S. & Kawashima, H. (1994) *J. Biol. Chem.* **269,** 27088–27092.
9. Birnbaumer, M., Seibold, A., Gilbert, S., Ishido, M., Barberis, C., Antaramian, A., Brabet, P. & Rosenthal, W. (1992) *Nature (London)* **357,** 333–335.
10. Lolait, S., O'Carroll, A.-M., McBride, O. W., Konig, M., Morel, A. & Brownstein, M. J. (1992) *Nature (London)* **357,** 336–339.
11. Acher, R. (1980) *Proc. R. Soc. London B* **210,** 21–43.
12. Mohr, E., Morley, SD & Richter, D. (1990) in *Neuropeptides and Their Receptors*, eds. Schwartz, T., Hilsted, L. M. & Rehfeld, J. F. (Munksgaard, Copenhagen), pp. 74–94.
13. Hruby, V. J. & Chow, M. S. (1990) *Annu. Rev. Pharmacol. Toxicol.* **30,** 501–534.
14. Manning, M. & Sawyer, W. H. (1993) *J. Receptor Res.* **13,** 195–214.
15. Probst, W. C., Snyder, L. A., Schuster, D. I., Brosius, J. & Sealfon, S. C. (1992) *DNA Cell Biol.* **11,** 1–20.
16. Sharif, M. & Hanley, M. R. (1992) *Nature (London)* **357,** 279–280.
17. Coughlin, S. R. (1994) *Curr. Opin. Cell Biol.* **6,** 191–197.
18. Baldwin, J. M. (1994) *Curr. Opin. Cell Biol.* **6,** 180–190.
19. Kaupmann, K., Bruns, C., Raulf, F., Weber, H. P., Mattes, H. & Lübbert, H. (1995) *EMBO J.* **14,** 727–735.

20. Kingston, R. E. (1987) in *Current Protocols in Molecular Biology*, eds Ausubel, F. M., Brent, R., Kingston, R. E., Moore, D. D., Smith, J. A., Seidman, J. G. & Struhl, K. (Greene, New York), pp. 9.0.1–9.5.6.
21. Teeter, M. M., Froimowitz, M., Stee, B. & DuRand, C. J. (1994) *J. Med. Chem.* **37,** 2874–2888.
22. Audigier, Y., Friedlander, M. & Blobel, G. (1987) *Proc. Natl. Acad. Sci. USA* **77,** 1496–1500.
23. Skatch, W. R., Shi, L.-B., Calayag, C., Frigeri, A., Lingappa, V. R. & Verkman, A. S. (1994) *J. Cell Biol.* **125,** 803–815.
24. Schöneberg, T., Liu, J. & Wess, J. (1995) *J. Biol. Chem.* **270,** 18000–18006.
25. Kojro, E., Eich, P., Gimpl, G. & Fahrenholz, F. (1993) *Biochemistry* **32,** 13537–13544.
26. Ufer, E., Postina, R., Gorbulev, V. & Fahrenholz, F. (1995) *FEBS Lett.* **362,** 19–23.
27. Chini, B., Moulliac, B., Ala, Y., Balestre, M.-N., Trumpp-Kallmeyer, S., Hoflack, J., Elands, J., Hibert, M., Manning, M., Jard, S. & Barberis, C. (1995) *EMBO J.* **14,** 2176–2182.
28. Higuchi, R., Krummel, B. & Saiki, R. K. (1988) *Nucleic Acids Res.* **16,** 7351- 7367.
29. Moulliac, B., Chini, B., Balestre, M.-N., Elands, J., Trumpp-Kallmeyer, S., Hoflack, J., Hibert, M., Jard, S. & Barberis, C. (1995) *J. Biol. Chem.* **270,** 25771–25777.
30. Regoli, D., Drapeau, G., Dion, S. & Di'Orleans-Juste, P. (1989) *Pharmacology* **38,** 1–15.
31. Fong, T. M., Huang, R.-R. C. & Strader, C. (1992) *J. Biol. Chem.* **267,** 25664- 25667.
32. Gether, U., Johansen, T. E., Snider, R. M., Lowe, J. A., III, Nakanishi, S. & Schwartz, T. W. (1993) *Nature (London)* **362,** 345–348.